

# MODELS AND SIMULATION OF BEAM HALO DYNAMICS IN HIGH POWER PROTON LINACS\*

Thomas P. Wangler

*Los Alamos National Laboratory, Los Alamos, NM 87545*

*Abstract*

We discuss the application of both multiparticle simulation techniques and analytical models known as particle-core models to the problem of understanding beam halo in high-power proton linacs. We emphasize the importance of multiparticle simulation including the space-charge forces as an essential tool for the description of the beam dynamics in a modern high-intensity proton linac. In addition, we have found that to understand the physics of beam halo, it has been necessary to supplement the simulations with a model known as the particle-core model.

## 1. INTRODUCTION

Within the past ten years, high-power proton linacs have been developed for several applications including neutron spallation sources, tritium production, and nuclear waste transmutation. The most challenging design parameters are those associated with the Accelerator for Production of Tritium (APT) linac [1]. APT is a CW proton linac with a final energy in the 1-GeV range. The average beam current is 100 mA, resulting in a final average beam power in the 100-MW range. Although the beam-physics regime is not very different than that for the LANSCE linac, which operates at Los Alamos, APT has an average current and beam power, which are a factor of 100 greater than for LANSCE. Consequently, designing for low beam loss to avoid radioactivation of the accelerator becomes a high priority to ensure that hands-on maintenance can be carried out, and that availability of the machine will remain high. To limit the average beam loss to the same absolute levels as have been achieved at LANSCE, the beam-dynamics design requirement for APT is to limit the beam loss to less than  $10^{-5}$  total or an average loss per unit length of less than  $10^{-8}/\text{m}$  for energies greater than 100 MeV. To accomplish this we must understand the causes and characteristics of the beam halo, since particles in the halo are those that may be lost on the accelerator walls.

## 2. MULTIPARTICLE SIMULATION

Multiparticle simulations are necessary for two important reasons. First, simulations are needed to describe the beam dynamics that depend on the nonlinear and time-dependent space-charge force, which is related to the evolving particle distribution. Second, simulations are needed to describe the effects of random linac errors or imperfections, which are treated using a Monte Carlo approach.

There is no consensus at present on a precise definition of the beam halo. Generally, the term halo describes the outer low-density edge of the beam in phase space that surrounds a dense central core. Typically, the halo particles are those that lie outside the phase-space boundary of an ellipse with the same shape as the rms emittance and an area of about 8 to 10  $\epsilon_{\text{rms}}$ , where  $\epsilon_{\text{rms}}$  is the rms emittance.

As a result of work done during the past few years, the main cause of beam-halo formation in high intensity proton-linac beams has been identified as arising from the space-charge forces that act in mismatched beams. In particular, this halo mechanism is the result of the coupling of collective oscillations to the motion of single particles. Because of the focusing provided in the three orthogonal directions, mismatch of the rms beam sizes generally excites some admixture of three collective envelope modes of the bunched beam, causing oscillations in the rms beam sizes. These envelope modes are shown in Fig. 1. Two modes have radial transverse oscillations where the transverse rms projections  $x_{\text{rms}}$  and  $y_{\text{rms}}$  move in phase; the longitudinal rms projection  $z_{\text{rms}}$  is either in phase with the transverse motion for a high-frequency or breathing mode, or out of phase for a low-frequency mode. The third envelope mode is the quadrupole mode, in which  $x_{\text{rms}}$  and  $y_{\text{rms}}$  are out of phase, and for this mode there is no longitudinal motion.

The focusing forces also produce oscillations of the individual particles, known as transverse or betatron oscillations, and longitudinal or synchrotron oscillations. When the oscillation frequency of a particle is half the frequency of one of the collective envelope modes, that particle can exchange energy with the mode through parametric resonance. The halo is formed mainly from those particles that are driven to large amplitudes through resonance with one or more of the envelope modes. Of the three envelope modes, the high and low frequency modes have already been identified as important for APT.

In the parameter regime of APT, the plasma parameter, or number of particles in a Debye sphere is much greater than unity, about  $10^6$ . In this regime the multiparticle Coulomb effect is accurately described by an average force, called the space-charge force, which is derivable from a potential that satisfies Poisson's equation. Discrete particle effects represent small fluctuations relative to the space-charge force, and are generally neglected. The space-charge force is calculated in computer codes by using the particle-in-cell (PIC) method, which is essentially a numerical method for solving the coupled Vlasov-Poisson equations that describe the simultaneous evolution of both the particle distribution and the space-charge fields. Before solving

Poisson's equation for a given time step, the charge distribution is transferred to a mesh using the particle distribution and including some form of smoothing to reduce numerical errors that are equivalent to artificial discrete-particle collisions.

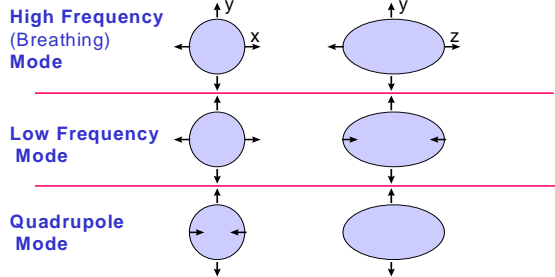


FIG. 1. Envelope modes of a mismatched bunched beam.

The simulation codes that are used for proton linacs typically use axial position as an independent variable, rather than time. For each particle in the bunch, the six phase-space variables, three position and three momentum coordinates, are tracked through the linac. Each time the space-charge subroutine is called, the particle coordinates must be transformed to positions corresponding to a fixed time, and then the particles are Lorentz transformed into the center-of-momentum frame of the bunch. A mesh is superimposed over the bunch and the particle charges are distributed among the mesh cells using an area weighting method that takes into account the position of each particle within its cell to determine the relative fraction of the particle charge that is assigned to each cell. This method provides the smoothing that was discussed earlier. Once the charge distribution has been determined, the electric field components are obtained on each grid point by numerical solution of Poisson's equation. The field components at the location of each particle are then obtained by interpolation of the field components from their values at the grid points. Two different PIC codes have been used, SCHEFF [2], a 2D r-z code, which uses an approximate correction for the effect of an elliptical transverse cross section, and a fully 3D PIC code called 3DPIC [3]. The 3DPIC code treats the 3D effects more accurately than SCHEFF, and up to  $10^7$  particles have been run in simulations on the CRAY T3E parallel computer. These two PIC codes have been compared for the APT linac design. Using  $10^5$  particles and with no random linac errors, excellent agreement has been obtained for all rms quantities and also for the maximum particle displacements. The SCHEFF routine has been benchmarked against the experimental measurements of rms beam properties at the LANSE proton linac; excellent agreement to within about 15% was observed [4].

The extent and the magnitude of beam halo in the linac is dependent on the machine errors or imperfections that produce mismatch. The simulation code uses the Monte Carlo approach to select errors within known tolerances. Many computer-simulation runs are required

from which the results may be combined to obtain probabilistic predictions for the expected beam distribution. For APT, we believe that linac errors could lead to effective mismatches in the range of 20% to 30%. The linac errors include misalignments and energy errors in the injected beam, RFQ higher multipoles and image-charge forces, quadrupole imperfections such as displacement, tilt, rotation, fringe fields, and higher multipoles, and cavity imperfections including phase and amplitude errors and tilts for the cavity fields. Fig. 2 shows the transverse beam size versus energy for APT for 20 runs with 100,000 particles for each run with different random errors. Shown are the aperture radius, the  $x_{rms}$  beam projection and the maximum displacement.

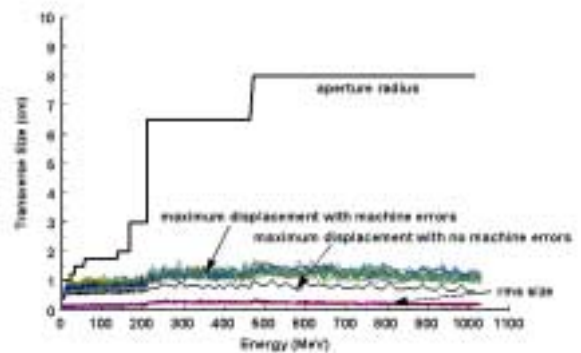


FIG. 2. Transverse rms size and maximum displacement versus energy along the APT linac for 20 simulation runs with different random linac errors and  $10^5$  particles per run. The aperture radius is shown for comparison, and the blue curve just below the 20 curves of maximum displacement is the maximum displacement when no random errors are present.

High performance parallel computing is becoming an important tool for linacs like APT for two reasons. First, the requirement that the total beam loss above 100 MeV must be limited to  $10^{-5}$  implies that to see losses at this level, simulation runs with greater than  $10^5$  particles per run are needed. Runs with  $10^7$  particles per run and greater will be helpful for obtaining even better statistical precision in the halo. Also, the use of parallel computing allows us to use the 3D PIC space-charge calculation, which is important to ensure that physics associated with 3D effects is not missed. Running  $10^7$  particles through the APT linac after the RFQ with the 3DPIC code, using 128 processors on a 64X64X128 grid, takes about 5.5 hours on the CRAY T3E computer. Fig. 3 shows the phase-space plots at the end of the APT linac for a  $10^7$  particle run on the CRAY T3E, including random linac errors.

### 3. PARTICLE-CORE MODEL

Computer simulation is an important tool but should not become a substitute for understanding the physics.

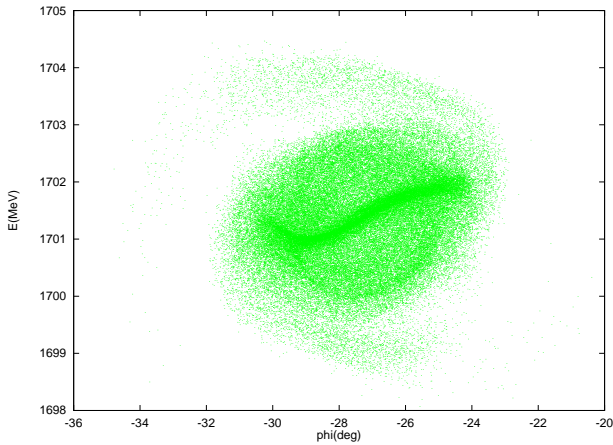


FIG. 3. Final longitudinal phase space plot (phase versus energy relative to the synchronous phase and energy) for a  $10^7$ -particle multiparticle simulation of the APT linac beam, including random linac errors, using the CRAY T3E parallel computer.  $10^5$  particles are included in the plot.

Models are important for providing additional understanding and insight. The particle-core model of beam-halo formation provides a framework for understanding the results of simulation, and provides scaling formulas that lead to guidelines for accelerator design. In this model the collective behavior is represented by the motion of the core. There are several particle-core models that have been constructed with different core geometries, including a 2-D continuous cylindrical beam [5,6], a spherical bunch, and a spheroidal bunch [7,8]. The latter model is the most representative model for a beam bunch in a linac. However, in this paper I discuss some results for the simpler case of a spherical bunch. In the spherical-bunch model, the beam core is represented by a uniform-density sphere in a uniform-focusing channel; the core experiences a linear external focusing force, as well as the defocusing effects from emittance plus the space-charge force. A mismatch of the initial core size is introduced that is symmetric in all three planes. This mismatch excites the radial breathing mode of the core. First, to understand the transverse particle dynamics, we study the motion of test particles that pass through the axis as they interact with the nonlinear space-charge field of the oscillating core and the applied linear external focusing force.

In the sphere model, the equation for the core motion is the envelope equation,

$$\frac{d^2 R}{ds^2} + k_0^2 R - \frac{(4\epsilon_{rms})^2}{R^3} - \frac{\kappa}{R^2} = 0, \quad (1)$$

where  $s$  is the axial coordinate,  $R$  is the core radius, the focusing force is represented by  $k_0$  which is also the wavenumber or phase advance per unit length of particle oscillations at zero current,  $\epsilon_{rms}$  is the rms unnormalized emittance, and

$$\kappa = \frac{q^2 N}{4\pi\epsilon_0 mc^2 \gamma^3 \beta^2}, \quad (2)$$

where  $q$ ,  $m$ , and  $\beta c$  are the charge, mass, and axial velocity of the particles, respectively,  $\gamma$  is the relativistic Lorentz factor,  $N$  is the number of particles per bunch,  $c$  is the speed of light, and  $\epsilon_0$  is the permeability of free space. For a matched beam, the core radius is constant, denoted by  $R = R_0$ . The motion of test particles that pass through the axis is governed by

$$\begin{aligned} \frac{d^2 x}{ds^2} + k_0^2 x - \frac{\kappa x}{R^3} &= 0, \quad x \leq 0, \\ \frac{d^2 x}{ds^2} + k_0^2 x - \frac{\kappa |x|}{x^3} &= 0, \quad x > 0. \end{aligned} \quad (3)$$

The net focusing force, including the space-charge term for a particle that always remains within the core, is represented by the wavenumber  $k$ , given by  $k^2 = k_0^2 - \kappa/R_0^3$ . For small mismatch oscillations the core breathing-mode wavenumber  $k_c$  can be expressed as  $k_c^2 = 3k_0^2 + k^2$ .

For the matched case, the core radius is constant, and there is no net change in the energy of a particle averaged over a complete period of the particle motion. For the mismatched case, the core radius oscillates, and particles can either gain or lose energy with each transit through the core. The particles experience a nonlinear space-charge force when they are outside the core and from Gauss' law this force is independent of the instantaneous size of the core. When the particles pass through the core, they are decelerated by the space-charge force as they approach the axis, and accelerated by the space-charge force as they leave the axis. The net space-charge impulse delivered to the beam is equal to the sum of a core-entrance contribution plus a core-exit contribution. These impulses may be either diminished or enhanced relative to the matched case, depending on whether the core radius is larger or smaller than the equilibrium value at the time the particle passed through. For example, if a particle enters the core when its radius is larger than the matched value, and exits when its radius is smaller than the matched value, a net energy impulse is delivered to the particle. Gluckstern [6], studying a particle-core model for a cylindrical beam, has shown that the effect of the core on the motion of the particles can be described by a nonlinear parametric resonance. The particles resonate with the core when the particle wavenumber  $\nu$  is related to the core breathing-mode wavenumber  $k_c$  by  $k_c = 2\nu$ . Note that  $\nu = k$  for particles that always remain within the uniform core, and  $\nu > k$  for particles with amplitude larger than the core radius, because of the reduced influence of the space-charge force for larger amplitudes. For nonzero beam current, one can show that the resonance condition requires that  $\nu > k$ , i.e. resonant particles must have amplitudes larger than the core radius. Thus, the decrease of the space-charge field with increasing displacement,

experienced by particles that are outside the core, produces an increase of the wavenumber  $\nu$  with amplitude so that the  $k_c = 2\nu$  resonant condition cannot be maintained as the amplitude increases; this effect limits the resonant amplitude growth. It is convenient to define two parameters, a space-charge tune-depression ratio  $\eta = k/k_0$ , and a mismatch parameter  $\mu = R_i/R_0$ , where  $R_i$  is the initial core radius.

Fig. 4 shows displacement versus axial distance for a particle driven by the resonance. The characteristics of the model are also displayed in the stroboscopic plot in Fig. 5, where a maximum amplitude is shown as the maximum displacement of the outer separatrix for particles in the resonance regions that are located between the inner and outer separatrices. By solving the equations of the sphere model numerically, we can determine the maximum amplitude for the resonantly driven particles. Fig. 6 shows a comparison of the maximum amplitudes from multiparticle simulations for an initial spherical Gaussian bunch with the maximum amplitudes obtained from the particle-core model. The agreement is good; the points from the simulation closely follow the general shape of the curves from the model and lie only slightly higher. Empirically we find that the maximum amplitude of the resonant particles satisfies an approximate formula

$$x_{\max} = x_{rms} (A + B|\ln(\mu)|) \quad (4)$$

where A and B are constants,

$$x_{rms}^2 \equiv \frac{\mathcal{E}_{rms}}{k_0 \beta \gamma} [1 + u]^{2/3}, \quad (5)$$

$$u = \frac{q^2 N}{20\sqrt{5}\pi\epsilon_0 mc^2 (k_0 \beta \gamma^3 \mathcal{E}_{n,rms}^3)^{1/2}}, \quad (6)$$

and  $\mathcal{E}_{n,rms}$  is the normalized rms emittance. These results from the sphere particle-core model provide the following guidelines for minimizing beam halo: good beam matching, small initial emittance, small number of particles per bunch (achieved for a given average current by choosing high bunch frequency), large  $k_0$  (strong focusing), and large  $\beta$  and  $\gamma$  (halo amplitudes are reduced at high energy).

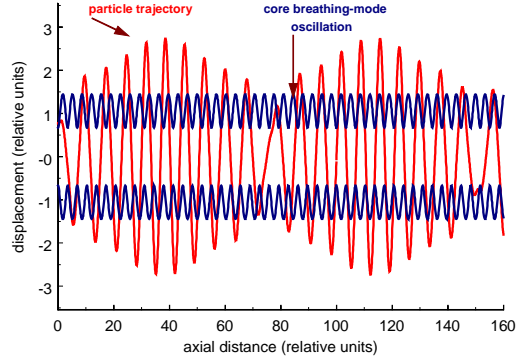


FIG. 4 Transverse displacement versus axial distance showing parametric resonance in the sphere particle-core model for a test particle with initial displacement of unity and initial divergence of zero. The envelope of the uniform-density spherical core is shown oscillating at about twice the frequency of the resonant test particle.

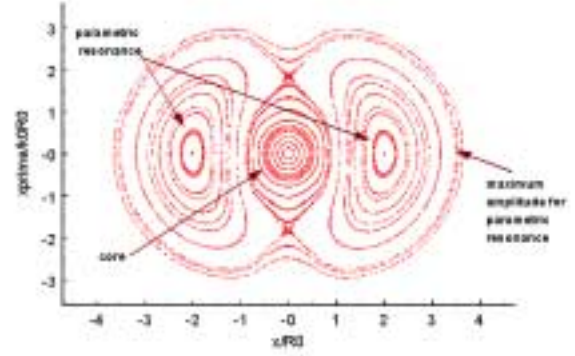


FIG. 5. Stroboscopic transverse phase-space plot for the sphere particle-core model for  $\mu=1.5$  and  $\eta = 0.5$ , showing the core region, the regions of parametric resonance, and the maximum displacement of the resonantly excited particles.

The sphere model presented here treats all three degrees of freedom the same. This model can be modified to account for nonlinear RF focusing in the longitudinal direction. If we assume that the core motion is approximately unaffected by the nonlinear focusing and that only the large amplitude test particles are affected, we can change the equation of motion for the test particles to

$$\frac{d^2 z}{ds^2} - \frac{qE_0 T (\cos(\phi_s - 2\pi z / \beta \lambda) - \cos(\phi_s))}{mc^2 \beta^2 \gamma^3} - \frac{\kappa z}{R^3} = 0, \quad z \leq R,$$

$$\frac{d^2 z}{ds^2} - \frac{qE_0 T (\cos(\phi_s - 2\pi z / \beta \lambda) - \cos(\phi_s))}{mc^2 \beta^2 \gamma^3} - \frac{\kappa z}{|z|^3} = 0, \quad z > R.$$

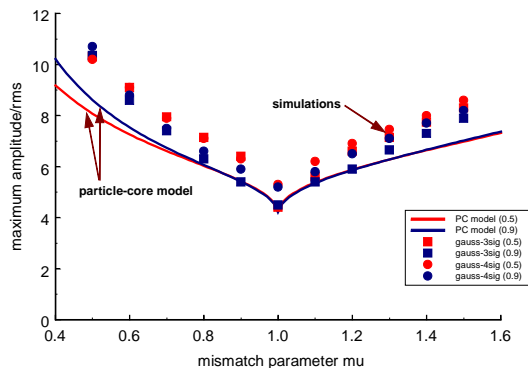


FIG. 6. Comparison of the maximum displacement from multiparticle simulations with the sphere particle-core model. The simulations are for initial spherical Gaussian bunches truncated at  $3\sigma$  and  $4\sigma$ ,  $\mu=1.5$ , and  $\eta = 0.5$  and  $0.9$ .

This change has a significant effect on the dynamics, by weakening the longitudinal focusing and reducing the particle frequencies for the large amplitude particles. The resulting stroboscopic plot for parameters near the APT parameter regime is shown in Fig. 7, for the parameter choices  $\mu=1.5$ ,  $\eta=0.5$ ,  $\phi_s=-30$  deg, and  $\phi_0=6.67$  deg, where  $\phi_s$  and  $\phi_0 = 2\pi R_0/\beta\lambda$  are the synchronous phase and the phase half width of the bunch, respectively.

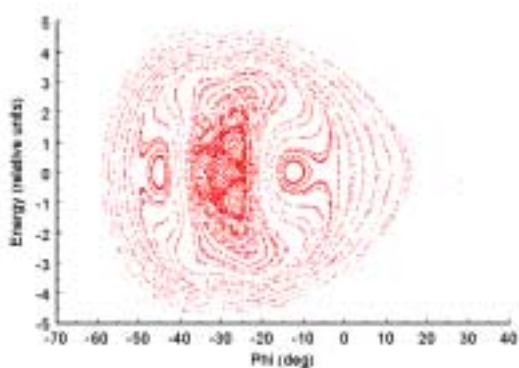


FIG. 7 Stroboscopic longitudinal phase-space plot of energy versus phase relative to the synchronous particle for the sphere particle-core model with a nonlinear rf force applied to the test particles and for parameters  $\mu=1.5$ ,  $\eta = 0.5$ ,  $\phi_s = -30$  deg and  $\phi_0 = 6.67$  deg.

While the sphere particle-core model exhibits many of the important features of the physics, it neglects some important effects which can only be treated properly by assuming a more realistic shape for the core geometry. Improvement is obtained by assuming a spheroidal core shape with radial and axial motion, where typically

$z_{rms} > x_{rms} = y_{rms}$ . This core geometry allows us to account for the presence of both the high and the low frequency modes. The spheroid model is being studied by both University of Maryland [7] and the Lawrence Livermore National Laboratory [8]. For the APT linac it is found that the high frequency mode primarily affects the transverse halo dynamics while the low frequency mode primarily affects the longitudinal halo dynamics.

## 4. CONCLUSION

Although multiparticle simulation is needed for a detailed description the beam halo, the particle-core model has been an indispensable complimentary tool. Combining these two methods has lead to a useful picture of the underlying physics of beam halo. Systematic studies using both simulation and the particle-core models describe the physics over the parameter regime of importance for high-power proton linacs.

## 5. ACKNOWLEDGMENTS

The author acknowledges support from the U.S. Department of Energy, and particularly wishes to thank John Barnard, Robert Gluckstern, and Robert Ryne for useful discussions.

## 6. REFERENCES

- 1 P.W. Lisowski in *Proc. 1997 Particle Accelerator Conf.*, Vancouver, British Columbia, Canada, (IEEE, Piscaraway, NJ, 1998), p. 3780.
- 2 T. P. Wangler, *Principles of RF Linear Accelerators* (John Wiley & Sons, Inc., New York, 1998), pp. 270-272.
- 3 R. Ryne, The U.S. Grand Challenge in Computational Accelerator Physics, to be published in *Proc. XIX International Linear Accelerator Conference (LINAC98)*, August 23-28, 1998, Chicago.
- 4 R. W. Garnett, R. S. Mills, and T. P. Wangler, *Proc. 1990 Linac Conf.*, Sept. 9-14, 1990, Albuquerque, NM, Los Alamos Report LA-12004-C, pp. 347-350.
- 5 For a discussion of the cylindrical beam model and for additional references see T.P.Wangler, K.R.Crandall, R.Ryne, and T.S.Wang, "Particle-Core Model for Transverse Dynamics of Beam Halo", to be published in *Physical Review Special Topics – Accelerators and Beams*.
- 6 R. Gluckstern, *Phys. Rev. Lett.* **73**, 1247 (1994).
- 7 R. L. Gluckstern, A. V. Fedotov, S. S. Kurennoy, and R. D. Ryne, *Phys. Rev. E.* **58**, 4977 (1998).
- 8 J. Barnard and S. Lund, *Proc. 1997 Particle Accelerator Conf.*, Vancouver, British Columbia, Canada, (IEEE, Piscaraway, NJ, 1998), p. 1929.